

## Thermophysical properties of lidocaine:thymol or L-menthol eutectic mixtures

María Molero-Sangüesa<sup>a</sup>, Isabel Jiménez-Omeñaca<sup>a</sup>, Fernando Bergua<sup>a,b</sup>, Héctor Artigas<sup>a,b</sup>, Carlos Lafuente<sup>a,b</sup>, Manuela Artal<sup>a,b,\*</sup>

<sup>a</sup> Departamento de Química Física, Facultad de Ciencias, Universidad de Zaragoza, Zaragoza, Spain

<sup>b</sup> Instituto Agroalimentario de Aragón - IA2 (Universidad de Zaragoza - CITA), Zaragoza, Spain

### ARTICLE INFO

#### Keywords:

Lidocaine  
Thymol  
L-menthol  
THEDES  
Thermophysical properties

### ABSTRACT

**Backgrounds:** A key objective of green chemistry is to obtain a broad database of thermophysical properties of liquid mixtures. Thus, the replacement of conventional solvents with ecological ones will be facilitated.

**Methods:** Herein, two eutectic systems with therapeutic properties are characterized. They are binary mixtures of lidocaine and thymol or l-menthol. Properties as solid-liquid equilibrium, density, speed of sound, refractive index, isobaric molar heat capacity, surface tension, and viscosity were determined at 0.1 MPa and several temperatures. From them, others derivatives were calculated. In addition, the phase diagram was correlated with NRTL model and the density and isobaric molar heat capacity were modelled with PC-SAFT equation of state.

**Significant findings:** Although the mixtures with l-menthol were almost ideal, a complex diagram owing the presence of stable and metastable phases. For these mixtures, the values of all measured properties were lower than those with thymol. Results indicated that PC-SAFT can be used to predict the thermodynamic behaviour of both systems in any working condition.

### 1. Introduction

Solvents are probably the most active research field in the green chemistry [1]. Its presence is essential both in chemical reactions and in processes of separation and purification of compounds. Traditional solvents are water and the volatile organic compounds (VOCs). The first has great advantages but its polarity and reactivity with many solutes are great drawbacks [2]. The VOCs are very effective but are not sustainable [3]. Therefore, the replacement of VOCs by eco-friendly solvents is the focus in many industries that seek to more sustainable processes. Several alternatives as sCO<sub>2</sub>, ionic liquids, and biomass-derived solvents have been proposed [4]. Eutectic solvents are the most recent neoteric solvents. They are mixtures (no pure compounds or pseudo-compounds) so it should be noted that their preparation is easy, efficient and does not produce waste. Although the term eutectic is old, the rise of these systems has occurred in the last 20 years. Fredrick Guthrie coined it in 1884 and defined it as "a lower temperature of liquefaction than that given by any other proportion" [5]. In 2004, Abbott et al. [6] studied ChCl/carboxylic acids mixtures and introduced the acronym corresponding to deep eutectic solvent (DES). Currently,

DESs are classified into five categories [7,8]. The first four have the general formula  $Cat^+X^-zY$  and the fifth are eutectic mixtures containing non-ionic compounds. Depending on the nature of its components, other acronyms are used. Literature collects interesting reviews on characteristics, types, properties, and applications of these mixtures [9–19]. In this paper, binary eutectic systems of type V containing active pharmaceutical ingredients (APIs) are studied. They have therapeutic properties so are called THEDESs [20].

Specifically, the APIs used here are lidocaine (L) and thymol (T) and l-menthol (M). Lidocaine (2-(diethylamino)-N-(2,6-dimethylfenil)acetamida) is a monocarboxylic acid amide prepared from the condensation of N,N-diethylglycine with 2,6-dimethylaniline. It was the first amine-amide local anesthetic, discovered in 1946 and marketed in 1949 [21, 22]. It is mainly used by dentists. In addition, L has the ability to block sodium channels and obstruct nerve signals, making it an effective antiarrhythmic and antiepileptic drug [21]. All this, together with its varied use as a surface anesthetic, makes its need in the market very important. It has been estimated at USD 1.19 billion by 2030 [23]. Lidocaine is present in a wide variety of formulations (injections, creams, gels, and inhalers for intubated patients) along with other active

\* Corresponding author.

E-mail address: [martal@unizar.es](mailto:martal@unizar.es) (M. Artal).

<https://doi.org/10.1016/j.jtice.2024.105631>

Received 10 April 2024; Received in revised form 11 June 2024; Accepted 15 June 2024

Available online 22 June 2024

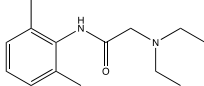
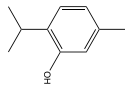
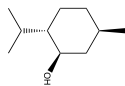
1876-1070/© 2024 The Author(s). Published by Elsevier B.V. on behalf of Taiwan Institute of Chemical Engineers. This is an open access article under the CC BY-NC-ND license (<http://creativecommons.org/licenses/by-nc-nd/4.0/>).

ingredients that enhance its effects. The best known is the eutectic mixture lidocaine-prilocaine sold as Emla®. Thymol (2-Isopropyl-5-metilfenol) and l-menthol (2-isopropyl-5-metilciclohexanol) are two terpenes that can be biosynthesized or extracted from plants. Both have biological activity and are known permeability enhancers [24–26]. They are Generally Recognized As Safe (GRAS) compounds according to the U.S Food & Drug Administration (FDA) classification [27]. The T and M structures differ only in the ring type; aromatic in the first and cyclic in the latter. This difference causes notable changes in the properties of their mixtures.

Several applications of the binary mixtures of L and T or M have been proposed as drug formulation, membranes development, and liquid-liquid extractions from aqueous solutions [28–35]. Despite this, these systems have been scarcely studied. An analysis of the structures by molecular dynamics was published by Abbas et al. [36,37]. Literature reports solid-liquid equilibria (SLE) data of both systems [30,38–41]. Also, four papers with values of some thermophysical properties as vapour pressure, density, and viscosity have been published [42–45]. No more data were found. The lack of experimental data on physicochemical properties is a serious problem for the definitive replacement of VOCs and the improvement of the sustainability of the processes [12, 14]. Tools such as the program for assisting the replacement of industrial solvents (PARIS III) [46] and the sustainable solvent selection and substitution software (SUSSOL) [47] provide the optimal substitute solvent for each process. This requires an extensive database of properties (density, phase equilibrium, refractive index, surface tension, heat capacity, viscosity, Hansen's parameters, solubility in water or partition coefficients). They are also necessary to apply thermodynamic models. It is unusual to find papers including both the experimental determination and modelling of a large number of properties for these solvents. We aim to fill this gap in the knowledge.

The purpose of this work is to characterize lidocaine and thymol or l-menthol eutectic mixtures of compositions (1:1) and (1:2) in mole ratio. Data of solid-liquid equilibria (SLE) and six thermophysical properties were measured and discussed. The effects of the temperature and composition on the properties were analysed and derived properties were calculated. Correlations between surface tension and critical temperature, or refractive index or viscosity were used. In addition, the validation of the perturbed chain-statistical associating fluid theory (PC-SAFT) equation of state (EoS) was performed for both systems to expand their use in the industry.

**Table 1**  
Chemicals used in this work.

Chemical (Acronym)	CAS No	Source	Purity <sup>a</sup>	<i>M</i> / g·mol <sup>-1</sup>	<i>T<sub>m</sub></i> / K	Structure
Lidocaine (L)	137-58-6	Sigma-Aldrich	>0.98	234.34	340.8/340.7 <sup>b</sup>	
Thymol (T)	89-83-8	Sigma-Aldrich	>0.985	150.22	322.5 <sup>c</sup>	
L-Menthol (M)	89-78-1	Sigma-Aldrich	>0.99	156.27	315.1 <sup>d</sup>	

<sup>a</sup> As stated by the supplier (mass fraction);

<sup>b</sup> [48].

<sup>c</sup> Ref. [49];.

<sup>d</sup> Ref. [50].

## 2. Experimental

### 2.1. Materials

The structures and characteristics of the pure compounds (L, T and M) are reported in Table 1. All of them were solid to 293 K. They were provided by Sigma–Aldrich and no purification processes were applied. The mixtures were prepared weighing each compound in adequate ratios with a PB210S Sartorius balance. The standard uncertainty was 1·10<sup>-4</sup> g. After, stirring and light heating (323 K) was applied until a homogeneous liquid was obtained.

The acronym, composition, molar mass and melting temperature of each THEDES studied are reported in Table 2. A Karl Fisher method (automatic titrator Crison KF 1S-2B) was used to determine the water content in the mixtures and a maximum value of 300 ppm was obtained.

### 2.2. Solid-Liquid equilibria

A differential scanning calorimeter (TA Instruments DSC Q2000) with an RCS refrigeration system was used to determine the solid-liquid equilibria (SLE). Indium was used as standard to calibrate the temperature and heat flow and the calculated uncertainty was  $u(T_m) = 0.5$  K. A liquid sample of 5 to 15 mg was weighed out and placed in an aluminium pan. For solid mixtures, it was preheated at a temperature above  $T_m$  to sure the crystallization into the device. After, the samples were cooled to 213–223 K at 3 K/min and then heated at the same scanning speed until 10 K above  $T_m$ . This scan rate was chosen regarding our previous studies

**Table 2**  
THEDESs studied: Acronym, composition, calculated molar mass, *M*, and melting temperature, *T<sub>m</sub>*.

THEDESs	Component 1	Component 2	Mole ratio	<i>M</i> <sup>a/</sup> / g·mol <sup>-1</sup>	<i>T<sub>m</sub></i> /K
LT11	Lidocaine	Thymol	1:1	192.28	—
LT12	Lidocaine	Thymol	1:2	176.48	—
LM11	Lidocaine	l-menthol	1:1	195.31	296.91 <sup>b</sup> / 295.77 <sup>c</sup> /305 <sup>d</sup> /312.2 <sup>e</sup>
LM12	Lidocaine	l-menthol	1:2	182.29	289.07 <sup>b</sup> / 275.54 <sup>e</sup>

<sup>a</sup>  $M = \sum M_i x_i$ .

<sup>b</sup> metastable  $\alpha$  – phase.

<sup>c</sup> metastable  $\beta$  – phase.

<sup>d</sup> [41].

<sup>e</sup> cocrystal, [40].

[50] where we did not observe any polymorphism in pure M. Different scanning rates have been reported in literature; for instance, Corvis et al. [40] used a rate of 10 K/min to obtain metastable L and M phases; Alhadid et al. [51] conducted DSC studies on the thymol and l-menthol system at rates 1, 2 and 5 K/min and Martins et al. [52] employed a heating ramp of 1 K/min to study eutectic systems based on terpenes and monocarboxylic acids. Both the eutectic melting temperature ( $T_{eu}$ ) and liquidus melting temperature ( $T_m$ ), we took the maximum value of the peak instead of the onset temperature. In the first case, the overlapping of eutectic peaks due to the polymorphism of M hinders the determination of the onset temperature which is the value usually reported. In the second one, the appearance of pretails and the asymmetry of the peaks prevent the obtention of the onset temperature.

### 2.3. Thermophysical properties

The devices used for thermophysical characterization of the studied mixtures are well-known and widely described in the bibliography. Table 3 collects the standard uncertainty in the temperature ( $u(T)$ ) and the calculated combined expanded uncertainties for each property ( $U_c(Y)$ ). Each apparatus was checked with benzene and the mean relative deviations ( $MRD(Y)$ ) obtained by comparison between our data and those from literature are listed in Table 3 [53,54]. It was assumed that the equilibrium state was reached when the property measure was stable. For each property, tabulated data were the average of two replicates. In all cases, the coefficient of variation had to be lower than the experimental uncertainty.

## 3. Results and discussion

### 3.1. Solid-Liquid equilibria

Knowing the solid-liquid phase diagram (SLE) of a solvent is essential for its implementation in any industrial application. It provides information about the stability of the solid and liquid phases as a function of temperature and composition. Additionally, in the case of eutectic mixtures, these diagrams can help to understand the physicochemical properties that characterize them. Also, the obtention of SLE phase diagram is the unique tool to distinguish a eutectic solvent from a deep eutectic solvent. In this work, when it has been possible, our experimental data have been compared to reported data to identify the detected thermal events and to analyze how can affect the experimental

**Table 3**  
Summary of the devices used in the thermophysical characterization.

Property	Devices	$u(T)/$ K	$U_c(Y)^a$	$MRD$ ( $Y$ ) <sup>b</sup> /%
$\rho$	Oscillating U-tube density meter, Anton Paar DSA 5000 <sup>c</sup>	0.005	0.05 kg·m <sup>-3</sup>	0.004
$u$	Sing-around technique in a fixed-path interferometer, Anton Paar DSA 5000 <sup>c</sup>	0.005	0.5 m·s <sup>-1</sup>	0.026
$n_D$	Standard Abbe refractometer, Abemat-HP refractometer Dr. Kernchen <sup>d</sup>	0.01	2·10 <sup>-5</sup>	0.007
$C_{p,m}$	Differential scanning calorimeter, TA Instruments DSC Q2000	0.5	1 %	0.028
$\gamma$	Drop volume tensiometer, Lauda TVT-2 <sup>d,e</sup>	0.01	1 %	0.21
$\nu$	Capillary viscosimeter Ubbelohde, Schoot-Geräte AVS-440	0.01	1 %	0.28

<sup>a</sup>  $k = 2(0.95$  level of confidence).

$$^b MRD(Y) = \frac{100}{n} \sum_{i=1}^n \frac{|Y_{i,lit} - Y_{i,exp}|}{Y_{i,exp}}$$

<sup>c</sup> Calibrated with two reference fluids: air and water MilliQ (resistivity of 18.2  $\mu\text{S}\cdot\text{cm}^{-1}$ ).

<sup>d</sup> Calibrated with water MilliQ (resistivity of 18.2  $\mu\text{S}\cdot\text{cm}^{-1}$ ) as reference fluid.

<sup>e</sup> 6 cycles of 6 drops per cycle were averaged.

method used. In relation to LT system, no thermal events were observed in the thermograms; An example is shown in Fig. S1a. In the literature few points have been reported and they correspond to compositions at the extremes of the diagram [30,33,39]. For LM, complex thermograms (Figs. 1a and S1b and c) were obtained owing to the presence of both stable and metastable SLE diagrams. The stable diagram is related to the presence of a cocrystal of equimolar composition, firstly reported by Corvis et al. [40]. When cocrystal is not formed, metastable SLE diagrams were found. Owing to the polymorphism exhibited by M and studied by us in a previous work [55] two different liquidus curves were obtained. As Corvis et al. [40] stated, in situ recrystallized samples lead to  $\beta$  metastable phase diagram. Therefore, in our case, we should observe thermal transitions related to  $\beta$  metastable, however we have identified thermal transitions of both stable and metastable phase diagrams (Fig. 1b). At rich M compositions, liquidus and eutectic points of  $\alpha$  and  $\beta$  metastable phases were obtained. The one identified as  $\alpha$ -phase had  $T_m$  higher than  $\beta$ -phase. At compositions close to equimolar composition, metastable mixtures transform to stable ones showing exothermic peaks at 280–290 K. Once metastable eutectic phases melt, they reformed the stable system. At rich L compositions, the same liquidus curves were detected for  $\alpha$  and  $\beta$  phases. Based on the experimental values, the NRTL model [56] was applied to LM system. The equations are reported in the supplementary file and the parameters are in Table S1. Our data (Table 2, Fig. 1b) agreed with those published by Corvis et al. [40]. The LM mixtures exhibited almost ideal behaviour. A metastable state with two phases was detected. The one identified as  $\alpha$ -phase had  $T_m$  higher than  $\beta$ -phase. The eutectic points obtained from NRTL model were:  $T_{eu,\alpha}=283.07$  K and  $x_{L,eu,\alpha}=0.39$ ;  $T_{eu,\beta}=272.88$  K and  $x_{L,eu,\beta}=0.35$ . The experimental values of  $T_{eu,\beta}$  were higher than the ones reported by Corvis et al. [40]. This fact is logical because we take the maximum peak as  $T_{eu}$  instead of onset temperature. In addition, two eutectic points related to stable SLE diagram were observed:  $T_{eu,1}=300.02$  K at  $x_L < 0.5$ , and  $T_{eu,2}=309.84$  K at  $x_L > 0.5$ . For comparison, in Fig. 2b are included the eutectic and invariant points from literature [40].

### 3.2. Thermophysical study

The properties determined were the density ( $\rho$ ), speed of sound ( $u$ ), refractive index ( $n_D$ ), isobaric molar heat capacity ( $C_{p,m}$ ), surface tension ( $\gamma$ ), and kinematic viscosity ( $\nu$ ). They were measured at  $p=0.1$  MPa and in the  $T$  range of 273.15 to 338.15 K. For the different properties, the lower and upper temperatures were different depending on the device limitations and  $T_m$  of each THEDES. All data are collected in several tables in the supplementary file (Tables S2-S7) and the corresponding figures (Fig. 2a–f) are given in the main manuscript. Data at 298.15 K are included in Table 4 for easier to follow the discussion.

The  $\rho$  of the studied mixtures with T were higher than those with M (Table S2). They were lower than that of water except for LT at low temperatures. The  $\rho$  difference with respect to that of water was less than 2.5 % for LT and varied between 4 and 8 % for LM. Therefore, only LM mixtures could be used effectively in liquid-liquid extraction applications with aqueous phase [45]. The measured values were compared with those found in the literature. The maxima deviations with data published by Xin et al. [43] were within of the experimental uncertainty: 0.28 kg/m<sup>3</sup> for LT11 and 0.03 kg/m<sup>3</sup> for LM12. However, our data at 298.15 K were up to 5 kg/m<sup>3</sup> lower than those of van Osch et al. [45] (Table 4). The trend of this property with concentration was the same for both systems but it was more pronounced for mixtures with M. For LT system, the  $\rho$  decreased slightly ( $< 5$  kg/m<sup>3</sup>) when T ratio doubled. For LM, the equimolar mixture was 18 kg/m<sup>3</sup> denser than the one richest in M throughout the  $T$  range studied. These results are owing the different geometry of both terpenes. The T has a flat structure due to the aromatic ring that occupies a smaller volume than the M cycle. Therefore, increasing the number of bulkier molecules must have a greater influence on the volumetric properties of the fluid. Being able to predict the

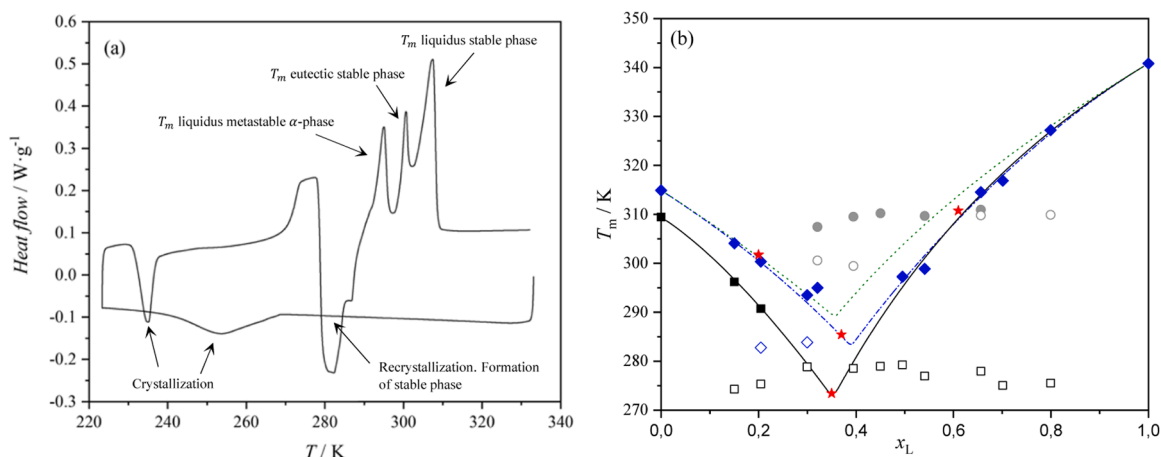


**Fig. 1.** Phase equilibria of LM system: (a) thermogram of LM12 obtained in this work; (b) SLE diagram. All data were obtained in this work except (★), Ref. [40]. (◆), metastable  $\alpha$ -phase; (■), metastable  $\beta$ -phase; (◇), metastable  $\alpha$ -phase; (□), metastable  $\beta$ -phase; (●), stable phase; (○), stable phase; (---), Ideal; (—•—) NRTL, metastable  $\alpha$ -phase; (—) NRTL, metastable  $\beta$ -phase.

density values of fluids at any composition and temperature is essential for its implementation in the industry. To this end, equations of state (EoS) such as PC-SAFT have been postulated as effective tools but must be previously validated. A brief summary of this model developed by Gross and Sadowski [57,58] is found in the supplementary file. In this EoS, each pure associated compound is characterized by five parameters and an association scheme. For T and M, the parameters were those published by Martins et al. [52]. For L, association parameters were taken from the literature and the rest were rescaled to fit its boiling point ( $T_b$ ) data [48]. Old parameters were obtained by Mahmoudabadi et al. [59] for lidocaine.HCl. The new parameters were validated by comparison between the boiling temperature published in the literature and the predicted one. The parameters and deviations are collected in Table 5. In the modelled of mixtures, mixing rules with a binary interaction parameter ( $k_{ij}$ ) are included. In our study, we have taken  $k_{ij}=0$ . Therefore, the model was used in its predictive version. To validate the PC-SAFT EoS for all THEDESS, our experimental  $\rho$  values were compared with those predicted ones. The mean relative deviations were  $MRD(\rho)=0.35\%$  and  $0.11\%$  for LT11 and LT12, and  $MRD(\rho)=0.76\%$  and  $0.49\%$  for LM11 and LM12. Overall, the model slightly overestimated  $\rho$  to a greater extent for the mixtures with M (Fig. S2a). The low deviations did not justify the introduction of a parameter  $k_{ij}\neq 0$ .

The variation of  $\rho$  with  $T$  was linear as expected in most liquids systems (Fig. 2a) and the coefficients are listed in Table 6. The isobaric expansivity ( $\alpha_p$ ), calculated with the following equation [60], allows quantifying the effect of  $T$  on  $\rho$ :

$$\alpha_p = -\frac{1}{\rho} \left( \frac{\partial \rho}{\partial T} \right)_p \quad (1)$$

The  $\alpha_p$  values at 298.15 K are reported in Table 4 and displayed at several temperatures in Fig. S3a. They were higher for LM system and increased with the terpene mole fraction. A comparison with similar mixtures of T and M with other compounds such as carboxylic acids is possible [49,50]. The mixtures studied here were denser and had higher expansion capacity than those. This fact could indicate strong terpenes-L interactions.

The more compact a material is the faster sound propagates through it. So, the  $u$  values of a fluid are related to its compaction. For the mixtures with T, they were about 50 m/s higher than those with M (Table S3). This property slightly increased with  $x_L$  in both systems and markedly decreased with  $T$  (Fig. 2b). The coefficients of the  $u - T$  linear

correlations are given in Table 6. The isentropic compressibility ( $\kappa_S$ ) is calculated from  $\rho$  and  $u$  data at each  $T$ . Subsequently, the free intermolecular length ( $L_f$ ) can be estimated using the constant of Jacobson ( $K$ ) [61]:

$$L_f = K\sqrt{\kappa_S} = (91.368 + 0.3565T)10^{-8} \sqrt{\frac{1}{\rho u^2}} \quad (2)$$

Table 4 collects  $\kappa_S$  and  $L_f$  data at 298.15 K. According to the above results, both properties were lower for the mixtures with T and decreased, very slightly for LT system, with  $x_L$  increasing. The  $L_f$  increased with  $T$  (Fig. S3b) due to the increase in the thermal agitation. The temperature coefficient for this property was similar for the four mixtures and the value was  $(\partial L_f/\partial T) = 2 \cdot 10^{-3} \text{Å} \cdot \text{K}^{-1}$ .

The  $n_D$  values of LT system were significantly higher than those for LM (Table S4). For the first, the effect of the composition on  $n_D$  was negligible. Also, a linear correlation with  $T$  was found for all cases as can be seen in Fig. 2c and Table 6. The molar refraction ( $R_m$ ), a property related to polarizability, can be calculated with the Lorentz-Lorentz equation [60]:

$$R_m = \left( \frac{n_D^2 - 1}{n_D^2 + 2} \right) V_m \quad (3)$$

Where  $V_m$  is the molar volume of the fluid at same  $p$  and  $T$ . Unlike  $n_D$ , the effect of the L ratio on  $R_m$  was stronger than the effect of terpene type (Table 4 and Fig. S3c). Thus, mixtures with a similar mole ratio presented similar  $R_m$  values and they were higher for the equimolar ones. Concerning similar mixtures with carboxylic acids previously published [49,50], the systems studied here exhibited an  $R_m$  up to 20 % higher than those. The aromaticity of the L molecule and the free electrons of the amine and amide groups would justify this result. The  $(V_m - R_m)$  difference is an estimation of the free volume ( $f_m$ ) of the system. The  $f_m$  percentages at 298.15 K were 69.5 % for both LT mixtures, and 70.9 % and 71.5 % for LM11 and LM12, respectively.

The measured  $C_{p,m}$  data of LM system were 8.5 % to 10 % higher than those of the LT in accordance with the higher molar mass of the former (Table S5). They ranged from 325  $\text{J} \cdot \text{mol}^{-1} \cdot \text{K}^{-1}$  of LT12 at 278.15 K to 429  $\text{J} \cdot \text{mol}^{-1} \cdot \text{K}^{-1}$  of LM11 at 338.15 K. The higher the temperature, the more energy the fluids store. Thus, the slope of  $C_{p,m} - T$  correlation must be positive as Fig. 2d shows. This property was also modelled with PC-SAFT EoS. The values were well predicted, especially those of the

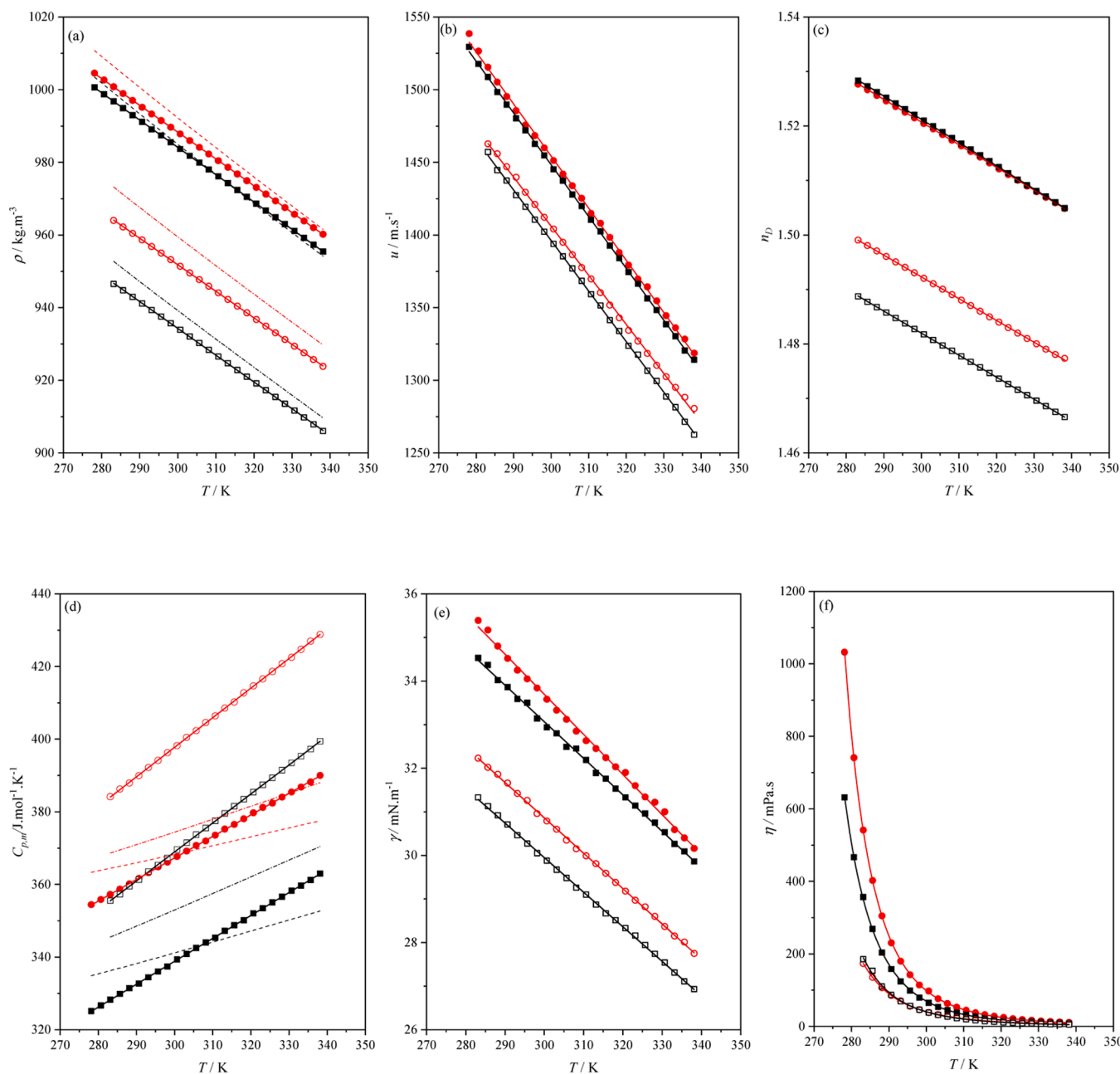


**Fig. 2.** Experimental thermophysical properties of THEDESs studied at several temperatures and at  $p = 0.1$  MPa. (a), density,  $\rho$ ; (b) speed of sound,  $u$ ; (c) refractive index,  $n_D$ ; (d) isobaric molar heat capacity,  $C_{p,m}$ ; (e) surface tension,  $\gamma$ ; (f) dynamic viscosity,  $\eta$ . (●), LT11; (■), LT12; (○), LM11; (□), LM12. Points, experimental values; (—), correlated data; (---), PC-SAFT EoS LT system; (- · -) PC-SAFT EoS LM system.

THEDES with T. The average deviations were  $MRD(C_{p,m}) = 1.5\%$  for LT and  $6.0\%$  for LM mixtures. A graphical comparison can be found in Fig. S2b.

Surface properties is related to the strength of the interactions within the fluid. Intermolecular forces must be weakened to increase the number of molecules at the fluid-air interface. The  $\gamma$  values of our systems were in agreement with the results from the above properties in which the L-T interactions were stronger than L-M (Table S6). For the first,  $\gamma$  was 10% higher than for the latter. The effect of  $T$  on  $\gamma$  was similar in both systems showing a linear correlation (Fig. 2e and Table 6). From  $\gamma - T$  data, thermodynamic properties such as the entropy of surface ( $\Delta S_s$ ) and enthalpy of surface ( $\Delta H_s$ ) can be calculated [60]:

$$\Delta S_s = - \left( \frac{\partial \gamma}{\partial T} \right)_p \quad (4)$$

$$\Delta H_s = \gamma - T \left( \frac{\partial \gamma}{\partial T} \right)_p \quad (5)$$

The higher the value of these properties, the more structured the fluid is. The calculated data indicated a high structuration within the mixtures with T (Table 4). Inside the liquid, the molecule is subjected to a symmetrical force field. Upon moving to the interface, the symmetry disappears and the molecule becomes polarized. The  $\gamma$  can be considered a consequence of this lack of symmetry and therefore, a measure of the polarization of molecules in the liquid surface. So, there is a correlation [62] between  $\gamma$  and the dielectric constant or  $n_D$  for liquids without strong hydrogen bonds (supplementary file). Table S8 reports the adjustment coefficients and shows high linearity with regression coefficients greater than 0.995. Considering that  $\gamma$  must be zero at the critical temperature ( $T_c$ ), different authors have proposed correlations



**Table 4**

Experimental and calculated properties<sup>a</sup> of THEDESs studied at  $T=298.15$  K and  $p = 0.1$  MPa.

Property	LT11	LT12	LM11	LM12
$\rho/\text{kg}\cdot\text{m}^{-3}$	989.66/989.64 <sup>b</sup> / 993.12 <sup>c</sup>	985.54/ 989.08 <sup>c</sup>	953.20	935.71/935.70 <sup>b</sup> / 939.18 <sup>c</sup>
$u/\text{m}\cdot\text{s}^{-1}$	1459.97	1454.74	1412.18	1402.15
$n_D$	1.52149	1.52204	1.49306	1.48274
$C_{p,m}/\text{J}\cdot\text{mol}^{-1}\cdot\text{K}^{-1}$	366	337	396	367
$\gamma/\text{mN}\cdot\text{m}^{-1}$	33.84	33.14	30.96	30.05
$\eta/\text{mPa}\cdot\text{s}$	114.33/111.3 <sup>b</sup> / 177.15 <sup>c</sup>	79.49/99 <sup>d</sup> / 122.05 <sup>c</sup>	46.06	46.20/45.91 <sup>b</sup> / 68.05 <sup>c</sup>
$\alpha_p/\text{kK}^{-1}$	0.746	0.763	0.767	0.788
$\kappa_s/\text{TPa}^{-1}$	474.05	479.46	526.06	543.59
$L_f/\text{Å}$	0.430	0.433	0.453	0.461
$R_m/\text{cm}^3\cdot\text{mol}^{-1}$	59.21	54.62	59.55	55.61
$\Delta S_S/\text{mN}\cdot\text{m}^{-1}\cdot\text{K}^{-1}$	0.091	0.084	0.081	0.080
$\Delta H_S/\text{mN}\cdot\text{m}^{-1}$	60.97	58.18	55.17	53.87
$E_{a,\eta}/\text{kJ}\cdot\text{mol}^{-1}$	63.96/67.67 <sup>b</sup> 48.5 <sup>d</sup>	62.30/	54.87	58.52/60.01 <sup>b</sup>

<sup>a</sup> Standard uncertainties are:  $u(T)=0.005$  K for  $\rho$  and  $u$ , 0.5 K for  $C_{p,m}$ , and 0.01 K for the rest of properties. The combined expanded uncertainties (0.95 level of confidence,  $k=2$ ) are  $U_c(\rho)=0.05$   $\text{kg}\cdot\text{m}^{-3}$ ;  $U_c(u)=0.5$   $\text{m}\cdot\text{s}^{-1}$ ;  $U_c(n_D)=2\cdot 10^{-5}$ ;  $U_c(C_{p,m})=1\%$ ;  $U_c(\gamma)=1\%$ ;  $U_c(\eta)=1\%$ ;  $U_c(\alpha_p)=0.04$   $\text{kK}^{-1}$ ;  $U_c(\kappa_s)=0.22$   $\text{TPa}^{-1}$ ;  $U_c(L_f)=0.005$   $\text{Å}$ ;  $U_c(R_m)=0.004$   $\text{cm}^3\cdot\text{mol}^{-1}$ ;  $U_c(\Delta S_S)=0.001$   $\text{mN}\cdot\text{m}^{-1}\cdot\text{K}^{-1}$ ;  $U_c(\Delta H_S)=0.06$   $\text{mN}\cdot\text{m}^{-1}$ .

<sup>b</sup> Ref. [43].

<sup>c</sup> Ref. [45].

<sup>d</sup> Ref. [42].

**Table 5**

PC-SAFT parameters used to model the studied THEDESs. The type 2B (one donor and one acceptor site) was considered as association scheme.

Compound	$m$	$\sigma/\text{Å}$	$\varepsilon/\text{K}$	$\kappa^{A_i B_i}$	$\varepsilon^{A_i B_i}/\text{K}$	$MRD(T_b)/\%$
Thymol <sup>a</sup>	4.012	3.816	290.22	0.0616	1660.0	0.4 <sup>d</sup>
Menthol <sup>a</sup>	4.152	3.903	262.40	0.0996	1785.6	0.3 <sup>d</sup>
Lidocaine <sup>b</sup>	6.320 <sup>c</sup>	3.770 <sup>c</sup>	285.85 <sup>c</sup>	0.01	2798.5	0.5 <sup>d</sup>

<sup>a</sup> Ref. [52].

<sup>b</sup> Ref. [59].

<sup>c</sup> this work.

<sup>d</sup> Ref. [48].

between both properties. Herein, we used the Guggenheim [63] and Eötvös [64] equations (supplementary file). In addition, EoSs as PC-SAFT allow estimating the critical temperatures and pressures ( $T_c$  and  $p_c$ ) of the systems. Although this model tends to overestimate the critical properties of the compounds, in our case the deviation of  $T_c$  of pure M was small (2.7 K). For T, it was higher (38 K) but the experimental value should be updated [49]. Furthermore, the thermodynamic properties of the mixtures were well predicted. The goodness of these results suggests that modelling of both critical loci could be acceptable. Table S9 lists the correlated and predicted values and Fig. 3 shows the critical loci.

The  $\eta$  indicates the ability of a system to flow. Table S7 reports the values measured in this work. Contrary to what is observed in other mixtures of these terpenes [49,50,55], the LT mixtures were more viscous than LM ones, especially at low  $T$  (Fig. 2f). For the first system, the  $\eta$  measured were very high and the values of the equimolar mixture were between 1.6 and 1.4 times higher than in the other. This ratio decreased with  $T$  increased. Increasing the  $x_T$  in the mixture increases the number of flatter molecules and decreases the number of I-T interactions. In consequence, the mobility of the fluid would be favoured. Also, the thermal agitation makes it difficult to maintain intermolecular interactions so the difference in fluidity of both mixtures is minimized at

**Table 6**

Fit parameters ( $A_Y, B_Y, C_Y$ ) and the regression coefficients,  $R^2$ , for the thermo-physical properties of the studied THEDESs.

Mixture	Property	$A_Y$	$B_Y$	$C_Y$	$R^2$
LT11	$\rho^a/\text{kg}\cdot\text{m}^{-3}$	1209.68	-0.7379		0.9999
	$u^a/\text{m}\cdot\text{s}^{-1}$	2529.30	-3.5833		0.9992
	$n_D^a$	1.64544	-4.2 $\cdot 10^{-4}$		0.9999
	$C_{p,m}^a/\text{J}\cdot\text{mol}^{-1}\cdot\text{K}^{-1}$	189.35	0.593		0.9999
	$\gamma^b/\text{mN}\cdot\text{m}^{-1}$	60.92	-0.091		0.9959
LT12	$\eta^c/\text{mPa}\cdot\text{s}$	0.03038	785.56	202.88	0.9999
	$\rho^a/\text{kg}\cdot\text{m}^{-3}$	1209.59	-0.7516		1
	$u^a/\text{m}\cdot\text{s}^{-1}$	2516.85	-3.5617		0.9999
	$n_D^a$	1.64917	-4.3 $\cdot 10^{-4}$		0.9999
	$C_{p,m}^a/\text{J}\cdot\text{mol}^{-1}\cdot\text{K}^{-1}$	149.51	0.631		0.9999
LM11	$\gamma^b/\text{mN}\cdot\text{m}^{-1}$	58.16	-0.084		0.9979
	$\eta^c/\text{mPa}\cdot\text{s}$	0.00623	1066.04	185.70	0.9998
	$\rho^a/\text{kg}\cdot\text{m}^{-3}$	1171.09	-0.7309		1
	$u^a/\text{m}\cdot\text{s}^{-1}$	2418.72	-3.3755		0.9994
	$n_D^a$	1.61218	-4.0 $\cdot 10^{-4}$		0.9999
LM12	$C_{p,m}^a/\text{J}\cdot\text{mol}^{-1}\cdot\text{K}^{-1}$	153.36	0.815		0.9999
	$\gamma^b/\text{mN}\cdot\text{m}^{-1}$	55.23	-0.081		0.9996
	$\eta^c/\text{mPa}\cdot\text{s}$	0.0336	705.38	200.67	0.9999
	$\rho^a/\text{kg}\cdot\text{m}^{-3}$	1155.43	-0.7371		0.9999
	$u^a/\text{m}\cdot\text{s}^{-1}$	2438.80	-3.4754		0.9997
LM12	$n_D^a$	1.60320	-4.0 $\cdot 10^{-4}$		0.9999
	$C_{p,m}^a/\text{J}\cdot\text{mol}^{-1}\cdot\text{K}^{-1}$	129.34	0.799		0.9999
	$\gamma^b/\text{mN}\cdot\text{m}^{-1}$	53.83	-0.080		0.9994
	$\eta^c/\text{mPa}\cdot\text{s}$	0.0194	765.39	199.83	0.9981

<sup>a</sup>  $Y = A_Y + B_Y T$ ; <sup>b</sup>  $Y = A_Y + B_Y T + C_Y T^2$ ; <sup>c</sup>  $Y = A_Y \exp\left(\frac{B_Y}{T - C_Y}\right)$ ; T in K.

high  $T$ . On the other hand, the viscosities for both LM mixtures were similar and the variation of  $\eta$  with the terpene concentration at  $T$  lower than 298.15 K was opposite to that in the previous system. These results could be explained considering that, although the I-M interactions were weaker than I-T ones, the structure of menthol caused greater steric hindrance. In the literature, we have found published  $\eta$  data of LT11 and LM12 from 293.15 to 353.15 K [43]. The maximum deviations with our data were 3.03 and 0.29 mPa·s, respectively. Also, our  $\eta$  data of LT12 in the  $T$  range from 293.15 to 328.15 K were compared with those published by Dietz et al. [42]. The maximum deviation was of 7.5 mPa·s. Again, data at 298.15 K reported by van Osch et al. [45] were very higher than the others (Table 4). Regarding the influence of  $T$  on  $\eta$ , the experimental data of all mixtures were correlated following the VFT exponential equation. The equation and coefficients  $A_Y$ ,  $B_Y$ , and  $C_Y$  are given in Table 6. The first is related to steric hindrance owing represents the  $\eta$  at  $T \rightarrow \infty$ . The others are used to calculate the activation energy for viscous flow ( $E_{a,\eta}$ ) [65]:

$$E_{a,\eta} = R \frac{\partial(\ln \eta)}{\partial\left(\frac{1}{T}\right)} = R \left( \frac{B_Y}{\left(\frac{C_Y}{T^2} - \frac{2C_Y}{T} + 1\right)} \right) \quad (6)$$

The results were in agreement with the structures of the compounds and with the above results. Thus,  $A_Y$  increased with  $x_L$  and was greater for the mixtures with M. Moreover,  $E_{a,\eta}$  values were higher in the mixtures with T, which shows that the I-T interactions were stronger than the I-M ones (Table 4, Fig. S3d). For LT system, the influence of  $T$  on  $E_{a,\eta}$  was more pronounced in the equimolar mixture showing that the interactions in LT12 were lower. For LM, the effect was similar for both compositions.

Finally, the Pelofsky and Murkerjee equations [66] correlate  $\eta$  and  $\gamma$  at similar  $p$  and  $T$ . The equations are found in the supplementary file and parameters are listed in Table S10. The obtained regression coefficients ranged from 0.90 to 0.95 for the former equation and 0.98 to 0.99 for the second.

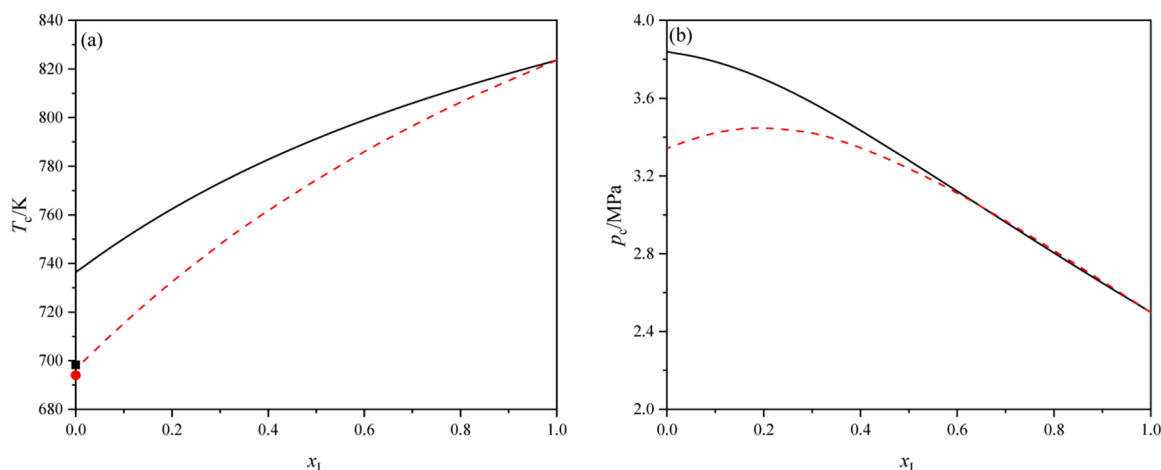


Fig. 3. Critical loci predicted with PC-SAFT EoS vs lidocaine molar ratio,  $x_L$ . (a) Critical temperature,  $T_c$ ; (b) Critical pressure,  $p_c$ . (—), LT; (---), LM. (■), pure T, ref. [48]; (●), pure M, ref. [48].

#### 4. Conclusions

Four therapeutic deep eutectic solvents (THEDESS) composed of lidocaine and thymol or l-menthol were studied. Melting temperatures and the following properties were determined at 0.1 MPa: density, speed of sound, refractive index, isobaric molar heat capacity, surface tension, and kinematic viscosity. From these values, derived properties were obtained and PC-SAFT EoS was applied.

The LM system exhibited an ideal phase behaviour and several states and phases were detected. The mixtures with T were more compact, structured, and viscous than those with M. The values of the measured properties decreased as the molar fraction of terpene increased. Correlations between surface tension and refractive index or viscosity showed good linearity with regression coefficients higher than 0.99 and 0.90, respectively. Finally, PC-SAFT EoS was validated in both systems. The maxima mean relative deviations concerning the experimental values were:  $MRD(\rho)=0.8\%$  and  $MRD(C_{p,m})=6\%$

#### CRediT authorship contribution statement

María Moreno: Investigation, Resources, Data curation. Isabel Jiménez-Omeñaca: Investigation, Resources, Data curation. Fernando Bergua Peña: Formal analysis – review & editing. Hector Artigas: Resources; Formal analysis. Carlos Lafuente: Project administration, writing – original draft. Manuela Artal: Validation, writing – original draft, writing – review & editing.

#### Data availability

All data generated or analysed in this study are included in the published article.

#### CRediT authorship contribution statement

María Molero-Sangüesa: Resources, Investigation, Data curation. Isabel Jiménez-Omeñaca: Resources, Investigation, Data curation. Fernando Bergua: Writing – review & editing, Formal analysis. Héctor Artigas: Resources, Formal analysis. Carlos Lafuente: Writing – original draft, Project administration. Manuela Artal: Writing – review & editing, Writing – original draft, Validation.

#### Declaration of competing interest

The authors declare that they have no known competing financial interests or personal relationships that could have appeared to influence

the work reported in this paper.

#### Acknowledgements

PLATON research group acknowledges financial support from Gobierno de Aragón and Fondo Social Europeo “Construyendo Europa desde Aragón” E31\_23R.

#### Supplementary materials

Supplementary material associated with this article can be found, in the online version, at doi:10.1016/j.jtice.2024.105631.

#### References

- [1] Anastas P, Eghbali N. Green chemistry: principles and practice. Chem Soc Rev 2010;39:301–12. <https://doi.org/10.1039/B918763B>.
- [2] Marcus Y. Applications of deep eutectic solvents. Springer, editor. deep eutectic solvents. Cham: Springer International Publishing; 2019. p. 1–11. [https://doi.org/10.1007/978-3-030-00608-2\\_4](https://doi.org/10.1007/978-3-030-00608-2_4).
- [3] Constable DJC, Curzons AD, Cunningham VL. Metrics to ‘green’ chemistry—which are the best? Green Chem 2002;4:521–7. <https://doi.org/10.1039/B206169B>.
- [4] Clarke CJ, Tu W-C, Levers O, Bröhl A, Hallett JP. Green and sustainable solvents in chemical processes. Chem Rev 2018;118:747–800. <https://doi.org/10.1021/acs.chemrev.7b00571>.
- [5] Guthrie FLII. On eutexia. The London, Edinburgh, and Dublin. Philosoph Mag J Sci 1884;17:462–82. <https://doi.org/10.1080/14786448408627543>.
- [6] Abbott AP, Boothby D, Capper G, Davies DL, Rasheed RK. Deep eutectic solvents formed between choline chloride and carboxylic acids: versatile alternatives to ionic liquids. J Am Chem Soc 2004;126:9142–7. <https://doi.org/10.1021/ja048266j>.
- [7] Smith EL, Abbott AP, Ryder KS. Deep eutectic solvents (DESS) and their applications. Chem Rev 2014;114:11060–82. <https://doi.org/10.1021/cr300162p>.
- [8] Abranches DO, Martins MAR, Silva LP, Schaeffer N, Pinho SP, Coutinho JAP. Phenolic hydrogen bond donors in the formation of non-ionic deep eutectic solvents: the quest for type v des. Chem Commun 2019;55:10253–6. <https://doi.org/10.1039/c9cc04846d>.
- [9] Martins MAR, Pinho SP, Coutinho JAP. Insights into the nature of eutectic and deep eutectic mixtures. J Solution Chem 2018. <https://doi.org/10.1007/s10953-018-0793-1>.
- [10] Oyouf F, Toncheva A, Henríquez LC, Grouniet R, Laoutid F, Mignet N, et al. Deep eutectic solvents: an eco-friendly design for drug engineering. ChemSusChem 2023;16. <https://doi.org/10.1002/cssc.202300669>.
- [11] Devi M, Moral R, Thakuria S, Mitra A, Paul S. Hydrophobic deep eutectic solvents as greener substitutes for conventional extraction media: examples and techniques. ACS Omega 2023;8:9702–28. <https://doi.org/10.1021/acsomega.2c07684>.
- [12] Abdelquader MM, Li S, Andrews GP, Jones DS. Therapeutic deep eutectic solvents: a comprehensive review of their thermodynamics, microstructure and drug delivery applications. Eur J Pharmaceut Biopharmaceut 2023;186:85–104. <https://doi.org/10.1016/j.ejpb.2023.03.002>.
- [13] Boateng ID. Evaluating the status quo of deep eutectic solvent in food chemistry. Potentials and limitations. Food Chem 2023;406. <https://doi.org/10.1016/j.foodchem.2022.135079>.

- [14] Hansen BB, Spittle S, Chen B, Poe D, Zhang Y, Klein JM, et al. Deep eutectic solvents: a review of fundamentals and applications. *Chem Rev* 2021;121:1232–85. <https://doi.org/10.1021/acs.chemrev.0c00385>.
- [15] Zhuang D, Chew KW, Teoh WY, Al-Maari MAS, Hizaddin HF, Alharthi S, et al. Extraction of phycocyanin from spirulina using deep eutectic solvent liquid biphasic system. *J Taiwan Inst Chem Eng* 2023;151:105125. <https://doi.org/10.1016/j.jtice.2023.105125>.
- [16] Vilas-Boas SM, Batista FRM, Dias RM, Coutinho JAP, Ferreira O, da Costa MC, et al. Deterpenation of citrus essential oil via extractive distillation using imidazolium-based ionic liquids as entrainers. *J Taiwan Inst Chem Eng* 2024;156:105367. <https://doi.org/10.1016/j.jtice.2024.105367>.
- [17] Zafarani-Moattar MT, Shekaari H, sadrmousavi Dizaj A, Asghari E. Effect of choline chloride based deep eutectic solvents on lithium perchlorate + propylene carbonate solutions: thermodynamic, transport, electrochemical and computational study. *J Taiwan Inst Chem Eng* 2021;128:20–9. <https://doi.org/10.1016/j.jtice.2021.09.007>.
- [18] Tang N, Liu L, Yin C, Zhu G, Huang Q, Dong J, et al. Environmentally benign hydrophobic deep eutectic solvents for palladium(II) extraction from hydrochloric acid solution. *J Taiwan Inst Chem Eng* 2021;121:92–100. <https://doi.org/10.1016/j.jtice.2021.04.010>.
- [19] Fahrina A, Yusuf M, Muchtar S, Fitriani F, Mulyati S, Aprilia S, et al. Development of anti-microbial polyvinylidene fluoride (PVDF) membrane using bio-based ginger extract-silica nanoparticles (GE-SINPs) for bovine serum albumin (BSA) filtration. *J Taiwan Inst Chem Eng* 2021;125:323–31. <https://doi.org/10.1016/j.jtice.2021.06.010>.
- [20] Aroso IM, Craveiro R, Rocha Â, Dionísio M, Barreiros S, Reis RL, et al. Design of controlled release systems for THEDES—Therapeutic deep eutectic solvents, using supercritical fluid technology. *Int J Pharm* 2015;492:73–9. <https://doi.org/10.1016/j.ijpharm.2015.06.038>.
- [21] Yang X, Wei X, Mu Y, Li Q, Liu J. A review of the mechanism of the central analgesic effect of lidocaine. *Medicine (Baltimore)* 2020;99:e19898. <https://doi.org/10.1097/MD.00000000000019898>.
- [22] Scriabini A. *Discovery and development of major drugs currently in use. pharmaceutical innovation: revolutionizing human health*. Philadelphia, PA: Chemical Heritage Press; 1999. p. 148–270.
- [23] Reports and Data. <https://www.reportsanddata.com/press-release/global-lidocaine-market-n.d>.
- [24] Marchese A, Orhan IE, Daglia M, Barbieri R, Di Lorenzo A, Nabavi SF, et al. Antibacterial and antifungal activities of thymol: a brief review of the literature. *Food Chem* 2016;210:402–14. <https://doi.org/10.1016/j.foodchem.2016.04.111>.
- [25] Herman A, Herman AP. Essential oils and their constituents as skin penetration enhancer for transdermal drug delivery: a review. *J Pharm Pharmacol* 2015;67:473–85. <https://doi.org/10.1111/jphp.12334>.
- [26] Cheng H, An X. Cold stimuli, hot topic: an updated review on the biological activity of menthol in relation to inflammation. *Front Immunol* 2022;13. <https://doi.org/10.3389/fimmu.2022.1023746>.
- [27] FDA. Food-additives-petitions/food-additive-status-list. [www.federalregister.gov/d/2022-19294](http://www.federalregister.gov/d/2022-19294) 2022:24–5.
- [28] Anstiss L, Weber CC, Baroutian S, Shahbaz K. Menthol-based deep eutectic solvents as green extractants for the isolation of omega-3 polyunsaturated fatty acids from Perna canaliculus. *J Chem Technol Biotechnol* 2023;98:1791–802. <https://doi.org/10.1002/jctb.7407>.
- [29] Dietz CHJT, Kroon MC, Di Stefano M, Van Sint Annaland M, Gallucci F. Selective separation of furfural and hydroxymethylfurfural from an aqueous solution using a supported hydrophobic deep eutectic solvent liquid membrane. *Faraday Discuss* 2018;206:77–92. <https://doi.org/10.1039/c7fd00152e>.
- [30] Wolbert F, Brandenbusch C, Sadowski G. Selecting excipients forming therapeutic deep eutectic systems - a mechanistic approach. *Mol Pharm* 2019. <https://doi.org/10.1021/acs.molpharmaceut.9b00336>.
- [31] Liu R, Hao J, Wang Y, Meng Y, Yang Y. A separation strategy of Au(III), Pd(II) and Pt(IV) based on hydrophobic deep eutectic solvent from hydrochloric acid media. *J Mol Liq* 2022;365:120200. <https://doi.org/10.1016/j.molliq.2022.120200>.
- [32] Kang L, Jun HW. Formulation and efficacy studies of new topical anesthetic creams. *Drug Dev Ind Pharm* 2003;29:505–12. <https://doi.org/10.1081/DDC-120018639>.
- [33] Kang L, Jun HW, Mani N. Preparation and characterization of two-phase melt systems of lidocaine. *Int J Pharm* 2001;222:35–44. [https://doi.org/10.1016/S0378-5173\(01\)00689-5](https://doi.org/10.1016/S0378-5173(01)00689-5).
- [34] Wang Y, Wang X, Wang X, Song Y, Wang X, Hao J. Design and development of lidocaine microemulsions for transdermal delivery. *AAPS PharmSciTech* 2019;20:63. <https://doi.org/10.1208/s12249-018-1263-1>.
- [35] Cabezas R, Duran S, Zurob E, Plaza A, Merlet G, Araya-Lopez C, et al. Development of silicone-coated hydrophobic deep eutectic solvent-based membranes for pervaporation of biobutanol. *J Memb Sci* 2021;637:119617. <https://doi.org/10.1016/j.memsci.2021.119617>.
- [36] Abbas UL, Qiao Q, Nguyen MT, Shi J, Shao Q. Molecular dynamics simulations of heterogeneous hydrogen bond environment in hydrophobic deep eutectic solvents. *AIChE J* 2022;68. <https://doi.org/10.1002/aic.17382>.
- [37] Abbas UL, Qiao Q, Nguyen MT, Shi J, Shao Q. Structure and hydrogen bonds of hydrophobic deep eutectic <sc>solvent-aqueous liquid-liquid</sc> interfaces. *AIChE J* 2021;67. <https://doi.org/10.1002/aic.17427>.
- [38] Kang L, Jun HW, McCall JW. Physicochemical studies of lidocaine-menthol binary systems for enhanced membrane transport. *Int J Pharm* 2000;206:35–42. [https://doi.org/10.1016/S0378-5173\(00\)00505-6](https://doi.org/10.1016/S0378-5173(00)00505-6).
- [39] Martins MAR, Silva LP, Jorge PS, Abranches DO, Pinho SP, Coutinho JAP. The role of ionic vs. non-ionic excipients in APIs-based eutectic systems. *Eur J Pharmaceut Sci* 2021;156:105583. <https://doi.org/10.1016/j.ejps.2020.105583>.
- [40] Corvis Y, Négrier P, Lazerges M, Massip S, Léger JM, Espeau P. Lidocaine/1-menthol binary system: cocrystallization versus solid-state immiscibility. *J Phys Chem B* 2010;114:5420–6. <https://doi.org/10.1021/jp101303j>.
- [41] Ma P, Toussaint B, Roberti EA, Scornet N, A Santos Silva, Castillo Henriquez L, et al. New lidocaine-based pharmaceutical cocrystals: preparation, characterization, and influence of the racemic vs. enantiopure cofomer on the physico-chemical properties. *Pharmaceutics* 2023;15:1102. <https://doi.org/10.3390/pharmaceutics15041102>.
- [42] Dietz CHJT, Creemers JT, Meuleman MA, Held C, Sadowski G, van Sint Annaland M, et al. Determination of the total vapor pressure of hydrophobic deep eutectic solvents: experiments and perturbed-chain statistical associating fluid theory modeling. *ACS Sustain Chem Eng* 2019;7:4047–57. <https://doi.org/10.1021/acssuschemeng.8b05449>.
- [43] Xin K, Roghair I, Gallucci F, van Sint Annaland M. Total vapor pressure of hydrophobic deep eutectic solvents: experiments and modelling. *J Mol Liq* 2021;325:115227. <https://doi.org/10.1016/j.molliq.2020.115227>.
- [44] Edgcomb JM, Tereshatov EE, Zante G, Boltoeva M, Folden CM. Hydrophobic amine-based binary mixtures of active pharmaceutical and food grade ingredients: characterization and application in indium extraction from aqueous hydrochloric acid media. *Green Chem* 2020;22:7047–58. <https://doi.org/10.1039/d0gc02452j>.
- [45] Van Osch DJGP, Dietz CHJT, Van Spronsen J, Kroon MC, Gallucci F, Van Sint Annaland M, et al. A Search for natural hydrophobic deep eutectic solvents based on natural components. *ACS Sustain Chem Eng* 2019;7:2933–42. <https://doi.org/10.1021/acssuschemeng.8b03520>.
- [46] Harten P, Martin T, Gonzalez M, Young D. The software tool to find greener solvent replacements, PARIS III. *Environ Prog Sustain Energy* 2020;39:1–7. <https://doi.org/10.1002/ep.13331>.
- [47] Sels H, De Smet H, Geuens J. SUSSOL-Using artificial intelligence for greener solvent selection and substitution. *Molecules* 2020;25:1–26. <https://doi.org/10.3390/molecules25133037>.
- [48] Linstrom P.J., Mallard W.G. NIST chemistry webbook, nist standard reference database number 69., Gaithersburg MD, 20899: 2020. <https://doi.org/10.18434/T4D303>.
- [49] Bergua F, Castro M, Muñoz-Embida J, Lafuente C, Artal M. Hydrophobic eutectic solvents: thermophysical study and application in removal of pharmaceutical products from water. *Chem Eng J* 2021;411. <https://doi.org/10.1016/j.cej.2021.128472>.
- [50] Bergua F, Castro M, Muñoz-Embida J, Lafuente C, Artal M. 1-menthol-based eutectic solvents: characterization and application in the removal of drugs from water. *J Mol Liq* 2022;352:118754. <https://doi.org/10.1016/j.molliq.2022.118754>.
- [51] Alhadid A, Jandl C, Mokrushina L, Minceva M. Experimental investigation and modeling of cocrystal formation in 1-menthol/thymol eutectic system. *Cryst Growth Des* 2021;21:6083–91. <https://doi.org/10.1021/acs.cgd.1c00306>.
- [52] Martins MAR, Crespo EA, Pontes PVA, Silva LP, Bülow M, Maximo GJ, et al. Tunable hydrophobic eutectic solvents based on terpenes and monocarboxylic acids. *ACS Sustain Chem Eng* 2018;6:8836–46. <https://doi.org/10.1021/acssuschemeng.8b01203>.
- [53] López N, Delso I, Matute D, Lafuente C, Artal M. Characterization of xylitol or citric acid:choline chloride:water mixtures: structure, thermophysical properties, and quercetin solubility. *Food Chem* 2020;306. <https://doi.org/10.1016/j.foodchem.2019.125610>.
- [54] Antón V, Artigas H, Muñoz-Embida J, Artal M, Lafuente C. Thermophysical study of 2-acetylthiophene: experimental and modelled results. *Fluid Phase Equilib* 2017;433:126–34. <https://doi.org/10.1016/j.fluid.2016.10.026>.
- [55] Bergua F, Castro M, Lafuente C, Artal M. Thymol+1-menthol eutectic mixtures: thermophysical properties and possible applications as decontaminants. *J Mol Liq* 2022;368:120789. <https://doi.org/10.1016/j.molliq.2022.120789>.
- [56] Renon H, Prausnitz JM. Local compositions in thermodynamic excess functions for liquid mixtures. *AIChE J* 1968;14:135–44. <https://doi.org/10.1002/aic.690140124>.
- [57] Gross J, Sadowski G. Perturbed-chain SAFT: an equation of state based on a perturbation theory for chain molecules. *Ind Eng Chem Res* 2001;40:1244–60. <https://doi.org/10.1021/ie0003887>.
- [58] Gross J, Sadowski G. Application of the perturbed-chain SAFT equation of state to associating systems. *Ind Eng Chem Res* 2002;41:5510–5. <https://doi.org/10.1021/ie010954d>.
- [59] Mahmoudabadi SZ, Pazuki G. Application of PC-SAFT EOS for pharmaceuticals: solubility, co-crystal, and thermodynamic modeling. *J Pharm Sci* 2021;110:2442–51. <https://doi.org/10.1016/j.xphs.2020.12.035>.
- [60] McNaught AD, Wilkinson A. *Compendium of Chemical Terminology. IUPAC recommendations*. 2nd editor. Cambridge: Blackwell Science; 1997.
- [61] Jacobson B. Ultrasonic velocity in liquids and liquid mixtures. *J Chem Phys* 1952;20:927–8. <https://doi.org/10.1063/1.1700615>.
- [62] Papazian HA. Correlation of surface tension between various liquids. *J Am Chem Soc* 1971;93:5634–6. <https://doi.org/10.1021/ja00751a008>.
- [63] Guggenheim EA. The principle of corresponding states. *J Phys Chem* 1945;13:253–61.



- [64] Shereshefsky JLL. Surface tension of saturated vapors and the equation of Eötvös. *J Phys Chem* 1930;35:1712–20. <https://doi.org/10.1021/j150324a014>.
- [65] Florindo C, Oliveira MM, Branco LC, Marrucho IM. Carbohydrates-based deep eutectic solvents: thermophysical properties and rice straw dissolution. *J Mol Liq* 2017;247:441–7. <https://doi.org/10.1016/j.molliq.2017.09.026>.
- [66] Pelofsky AH. Surface Tension-Viscosity Relation for Liquids. *J Chem Eng Data* 1966;11:394–7. <https://doi.org/10.1021/je60030a031>.